Research Article | Vol. 28, No. 10 / 11 May 2020 / Optics Express 14357
Optics EXPRESS

Convolutional neural network-based signal demodulation method for NOMA-PON

BANGJIANG LIN,[1] HUI YANG,[2,4] RUI WANG,[2] ZABIH GHASSEMLOOY,[3] AND XUAN TANG[1,5]

[1]Quanzhou Institute of Equipment Manufacturing, Haixi Institutes, Chinese Academy of Sciences, China
[2]School of Information Science and Technology, Southwest Jiaotong University, Chengdu, China
[3]Optical Communications Research Group, Faculty of Engineering and Environment, Northumbria University, UK
[4]yanghuifly@home.swjtu.edu.cn
[5]xtang@fjirsm.ac.cn

Abstract: Non-orthogonal multiple access (NOMA) is a promising scheme for flexible passive optical networks (PONs), which provides high throughput and overall improved system performance. NOMA with the successive interference cancellation (SIC)-based receiver, which is used to detect the multiplexed signal in a sequential fashion, requires perfect channel state information and suffers from the error propagation problem. In this paper, we propose a convolutional neural network (CNN) based signal demodulation method for NOMA-PON, which performs channel estimation and signal detection in a joint manner. The CNN is first trained offline using the captured data for a given received optical power and then used to recover the data stream directly in the online mode. We show by experimental demonstration that, the proposed CNN-based receiver (Rx) outperforms the conventional SIC-based Rx and is more robust to the nonlinear distortion. We show that for the CNN-based system with 20 km optical fiber, the required received optical power levels at a bit error rate (BER) of 1×10^{-3} are lower by 4, 3 and 2.5 dB for power allocation ratios of 0.16, 0.25, 0.36, respectively compared with SIC-based system. In addition, the BER performance of CNN deteriorates considerably less with non-linear distortion compared with SIC.

1. Introduction

The non-orthogonal multiple access (NOMA) scheme is seen as a potential option in communication systems in order to increase the system throughput and user fairness [1]. Fundamental works on the rate region, bit error rate (BER) performance and resource allocation schemes have been carried out to improve the reliability and efficiency of NOMA-based wireless systems [2–4]. Recently, NOMA has been introduced into optical communication systems. In [5], a digital non-orthogonal multiplexing scheme was proposed to increase the spectrum efficiency of dual polarization coherent optical orthogonal frequency division multiplexing (OFDM) systems. In [6,7], NOMA based visible light communication (VLC) systems were experimentally demonstrated with higher throughput. NOMA is shown to be particularly suitable for indoor VLC systems, where users experience different channel gains. In [8–10], NOMA was adopted in a flexible passive optical network (PON) in order to improve the performance and reliability of system. In traditional orthogonal multiple access (OMA)-based PON, it is challenging to provide high-speed services to the entire optical network units (ONUs) since the service quality is mostly affected by the ONU with the highest path loss. Whereas, NOMA-PON can provide high quality of service and improved sum rate. In NOMA systems, the multiplexed signals are detected using a successive interference cancellation (SIC)-based receiver (Rx) in a sequential manner, which induces the error propagation (EP) problem. Thus, leading to degradation of the system bit error rate (BER) performance and increasing user's unfairness [11]. To mitigate the EP, a SIC-free

#392535 https://doi.org/10.1364/OE.392535
Journal © 2020 Received 10 Mar 2020; revised 21 Apr 2020; accepted 21 Apr 2020; published 27 Apr 2020

Optics EXPRESS

NOMA scheme was proposed in [12]. In addition, the channel state information (CSI) has a great impact on the performance of NOMA systems [6]. Therefore, employing accurate channel estimation (CE) methods is desirable in order to acquire perfect CSI. In [13], a novel linear estimator was designed to acquire the CSI, which aimed at maximizing the average signal to interference and noise ratio (SINR) of the strong user.

In recent years, machine learning especially neural network (NN) has become very popular and been introduced in optical communications for monitoring the optical signal to noise ratio (OSNR) [14], modulation format recognition [14], nonlinearity mitigation [15] and CE [16–17], etc. In [16], the NN-based equalizer was used to mitigate both linear and nonlinear distortion in a 100 Gb/s PON system. In [17], a memory controlled deep long short-term memory (LSTM) NN-based post-equalizer was proposed to mitigate the transmission impairment in pulse amplitude modulation VLC systems. In [18], a LSTM network was proposed to detect the channel characteristics automatically for a typical NOMA system. In this paper, we propose a convolutional neural network (CNN)-based signal demodulation method for NOMA-PON, where the received multi-users' signals are decoded in a one-shot process without CE. The proposed scheme offers enhanced flexibility with reduced NOMA demultiplexing latency and no requirement for the CSI. We show by experimental demonstration that, the proposed CNN-based Rx with generalization ability and high robustness against nonlinear distortion can significantly improve the BER performance of NOMA-PON.

2. Theory

Fig. 1 shows the schematic diagram of downstream NOMA-PON with a CNN-based demodulator. At the optical line terminal (OLT), the data stream $d_i(t)$ for the source for each ONU is converted into 4-quadrature amplitude modulation (QAM) prior to being encoded into an OFDM symbol. Following preamble insertion (for frame synchronization) and power allocation, OFDM signals are combined together, which is given as:

$$\mathbf{X} = \sum_{i=1}^{N} \sqrt{p_i}\mathbf{X}_i, \tag{1}$$

where p_i and $\mathbf{X}_i$ are the allocated power and the transmitted frequency domain signals for the i-th ONU, respectively and N is the number of ONU. The total transmitted data bit on each subcarrier is $2N$. $\mathbf{X}_i = [X_{i,1}, X_{i,2}, \ldots X_{i,M}]^T$, where M is the number of subcarriers (i.e., the sizes of discrete Fourier transform (DFT) and inverse DFT (IDFT)) and T denotes the matrix transposition. The digital OFDM signal is applied to a digital-to-analog converter (DAC) the output of which is used for external modulation (EM) of a laser source. The optical signal is launched into a single mode fiber and then distributed to all ONUs via an optical distribution network (ODN) following transmission. For each ONU, the output of an optical Rx is applied to an analog to digital converter (ADC). Following frame synchronization and cyclic prefix (CP) removal, the output of DFT is given as:

$$\mathbf{Y} = \mathbf{H} \times \sum_{i=1}^{N} \sqrt{p_i}\mathbf{X}_i + \mathbf{W}, \tag{2}$$

where $\mathbf{W}$ is the noise vector, $\mathbf{H} = \mathrm{diag}(H_1, H_2, \ldots, H_M)$ and H_i is the frequency channel response for the i-th subcarrier. Finally, the regenerated NOMA signal (i.e., $\mathbf{Y}$) is demodulated using the CNN-based demodulator.

Fig. 2 shows the structure of the CNN-based demodulator, which is composed of three convolutional layers of Conv-1, Conv-2 and Conv-3. The input signal $\mathbf{Y}$ to Conv-1 is firstly divided into real and imaginary components (i.e., $\mathbf{Y}^{\mathrm{R}}$ and $\mathbf{Y}^{\mathrm{I}}$). $\mathbf{Y}^{\mathrm{R}}$ and $\mathbf{Y}^{\mathrm{I}}$ convolute with M

Optics EXPRESS

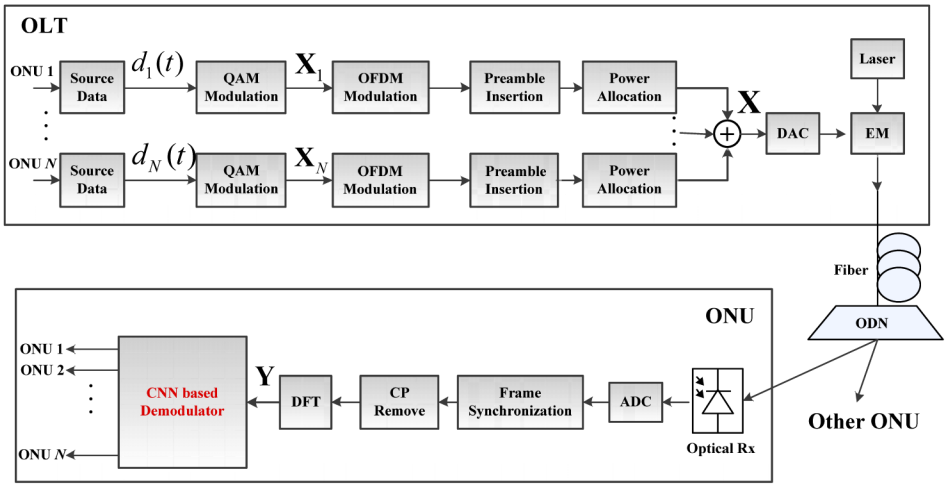

Fig. 1. A schematic block diagram of NOMA-PON system employing a CNN-based demodulator.

kernels the output of which is given as:

$$\mathbf{S}_i^1 = (\mathbf{Y}^{\mathrm{R}} + \mathbf{Y}^{\mathrm{I}}) * \mathbf{K}_{1,i} + b_{1,i}\,, \tag{3}$$

where $\mathbf{K}_{1,i}$ denotes the i-th kernel of Conv-1, $i = 1, 2, \ldots, M$ and $b_{1,i}$ is the bias of $\mathbf{K}_{1,i}$. In order to improve the training performance, we have included batch normalization for the proposed network, which is expressed as:

$$\mathbf{S}_i^2(j) = \frac{\mathbf{S}_i^1(j) - \mathrm{E}[\mathbf{S}_i^1(j)]}{\sqrt{\mathrm{Var}[\mathbf{S}_i^1(j)] + \varepsilon}} * \gamma + \beta, \tag{4}$$

where $j = 1, 2, \ldots, M$, β and γ are the learnable parameters. The final output of Conv-1 is given as:

$$\mathbf{Z}_{1,i}(j) = \max(0, \mathbf{S}_i^2(j)). \tag{5}$$

The structure of Conv-2 with the input $\mathbf{Y}^2 = [\mathbf{Z}_{1,1}, \mathbf{Z}_{1,2}, \ldots, \mathbf{Z}_{1,M}]$ is similar with Conv-1, which contains M kernels (i.e., $\mathbf{K}_{2,i}$, $i = 1, 2, \ldots, M$). $\mathbf{Y}^2$ first convolute with $\mathbf{K}_{2,i}$ as follows:

$$\mathbf{S}_i^3 = \sum_{j=1}^{M} \mathbf{Z}_{1,j} * \mathbf{K}_{2,i} + b_{2,i}\,, \tag{6}$$

where $b_{2,i}$ is the bias of $\mathbf{K}_{2,i}$. $\mathbf{S}_i^3$ is also batch normalized as follows:

$$\mathbf{S}_i^4(j) = \frac{\mathbf{S}_i^3(j) - E[\mathbf{S}_i^3(j)]}{\sqrt{Var[\mathbf{S}_i^3(j)] + \varepsilon}} * \gamma + \beta. \tag{7}$$

The final output of Conv-2 is given as:

$$\mathbf{Z}_{2,i}(j) = \max(0, \mathbf{S}_i^4(j)). \tag{8}$$

Conv-3 contains $2N$ kernels with the input $\mathbf{Y}^3 = [\mathbf{Z}_{2,1}, \mathbf{Z}_{2,2}, \ldots, \mathbf{Z}_{2,M}]$. $\mathbf{Y}^3$ first convolute with $\mathbf{K}_{3,i}$ ($i = 1, 2, \ldots, 2N$) as follows:

$$\mathbf{S}_i^5 = \sum_{j=1}^{M} \mathbf{Z}_{2,j} * \mathbf{K}_{3,i} + b_{3,i}, \tag{9}$$

Optics EXPRESS

where $b_{3,i}$ is the bias of $\mathbf{K}_{3,i}$. Sigmoid function is used as the final activation function, the final output of Conv-3 is given as:

$$\mathbf{Z}_{3,i}(j) = \text{sigmoid}\,(\mathbf{S}_i^5(j)). \tag{10}$$

After the three convolutional layers, the output is fed into a hard decision module. If $\mathbf{Z}_{3,i}\,(j) > 0.5$, the received i-th data bit on j-th subcarrier is 1, otherwise it is 0. The loss function of the network is mean square error (MSE) given as:

$$MSE = \sum_{j=1}^{M}\sum_{i=1}^{2N}(\text{sigmoid}\,(\mathbf{Z}_{3,i}(j)) - S_{i,j}), \tag{11}$$

where $S_{i,j}$ denotes the i-th transmitted data bit (0 or 1) on the j-th subcarrier. Note that, by means of training, the MSE can be minimized step-by-step and therefore the CNN-based demodulator output representing the original transmitted data bit streams. The training network is based on the backpropagation where the loss function is back propagated to update the weight parameters by mini-batch gradient descent with Rmsprop optimization with a batch size of 300-1000. To increase the training efficiency and reduce the convergence speed, Rmsprop optimization will adaptively adjust the learning rate depending on the first and second order moment estimations. Note, in the convolutional layers, we have adopted a higher number of kernels but with smaller dimension, which makes the network has more non-linear changes, thus leading to stronger learning capabilities and reduced computational complexity [19]. For all the convolutional layers in Fig. 2, the kernel size and the stride are both set to 1. This implies that, each input symbol is treated individually, since the symbols are memoryless. Compared with traditional SIC, the NN based demodulator has higher computational complexity. Note, other NNs, such as fully connected NN, LSTM network can also be used to decode the NOMA signal with similar transmission performance. However, the convergence speed of the LSTM is much slower than that of fully connected NN and CNN. Due to its characteristic of sparse connection and weight sharing, CNN can use fewer training parameters to achieve the same performance compared to fully connected NN. As such, the CNN has the advantages of low complexity, high convergence speed and easy to optimize the network model, thus being chosen to decode the NOMA-OFDM signal.

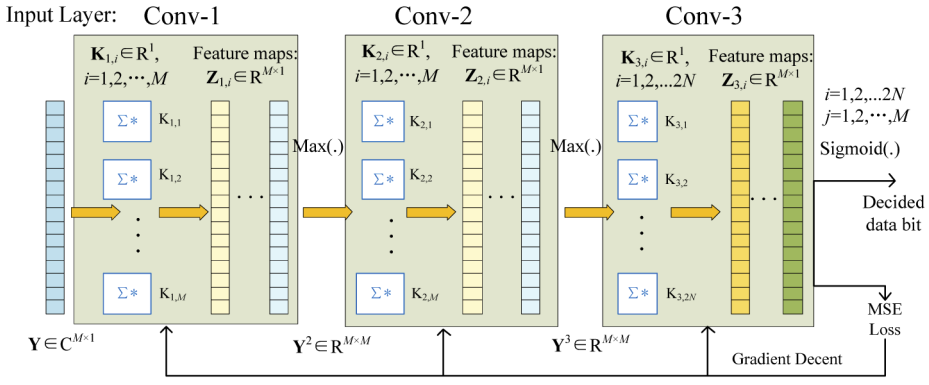

Fig. 2. The structure of CNN based demodulator.

3. Experiment setup and results

In this section, we investigate the transmission performance of the proposed CNN-based Rx, using the schematic diagram of experiment setup shown in Fig. 3. At the OLT, the two data sources

Optics EXPRESS

(generated randomly in MATLAB) are mapped into 4-QAM and then encoded into OFDM symbols. The sizes of IDFT and CP are 64 and 8, respectively. The symbol rate of each OFDM signal is 3.3 GBaud/s. The two OFDM signals with pre-allocated powers are combined together prior to being up-converted to a radio frequency (RF) carrier signal with a frequency of 2.5 GHz. This is done in order to ensure that, the NOMA signal to be real value. An arbitrary waveform generator (AWG, Tektronix 70002A) with a sampling rate of 10 GS/s is used for generation of the digital NOMA signal, the output of which is used for EM of a laser (KG-DFB-15-10-FA) using a Mach-Zehnder modulator (MZM). The modulated light signal is fed into a single mode fiber (SMF) for distribution to ONU1&2 via a 50/50 optical coupler and a variable optical attenuator. At the ONU, the outputs of the optical Rx (i.e., regenerated electrical NOMA) are captured using a digital oscilloscope (Tektronix DPO71604C, 16 GHz bandwidth and maximum sampling rate of 100 GS/s) with a sampling rate of 10 GS/s for off-line processing (i.e., decoding, etc.) using MATLAB and Python. Note, the NOMA signal is firstly down-converted to the baseband and then decoded as shown in Figs. 1 and 2. In the experiment, both the data sets for offline training and online deployment are generated randomly by the random function of MATLAB. Specifically, in the training stage, we use 8 random seeds generated from system time to generate the binary data for NOMA modulation, resulting a length of 48000 NOMA symbols. At the receiver, data augmentation method is used. 10000 of 48000 captured NOMA symbol is randomly selected (the selecting index is also generated using a random seed from the system time) to fed into the CNN to train the network for each training epoch. At the online deployment, we also use 8 random seeds generated from system time to generate the binary data for NOMA modulation. The length of NOMA signal is 48000. Data augmentation method is also used for the captured NOMA symbols for testing. We have confirmed via simulation that our CNN is unable to characterize the random sequences we used. All the key system parameters adopted are provided in Table 1.

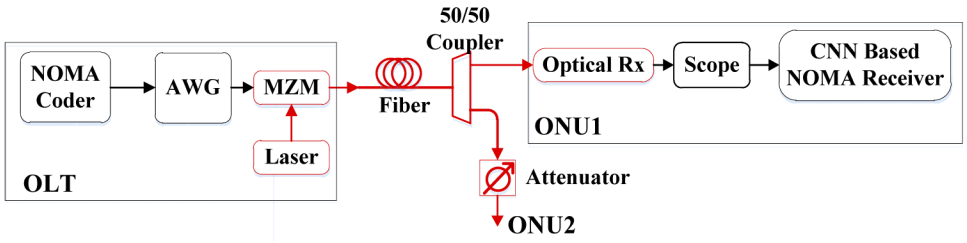

Fig. 3. Experiment setup for NOMA-PON with two ONUs.

Figures 4–6 show the average BER performance as a function of the received optical power P_r after transmission over a 20 km SMF for downstream NOMA-PON with a transmit optical power P_t of 0 dBm using SIC- and CNN-based Rxs for power allocation ratios (PARs) of 0.16, 0.25, 0.36, respectively. At the training stage, the NOMA signals were captured for the same P_r. Note, CNN has a generalization ability (i.e., CNN trained at a given P_r can also be used to detect other NOMA signals captured at different P_r). We found that, the network trained at higher P_r can only learn about the perfect signal demodulation without knowing about the linear and nonlinear distortions. Whereas the network trained with lower P_r is more susceptible to the noise. The CNN-based Rx performs best when the network is trained for a range of P_r (i.e., -11 to -8 dBm, -13 to -10 dBm and -14 to -9 dBm for the PAR values of 0.16, 0.25 and 0.36, respectively). To achieve a BER of 1×10^{-3}, the required P_r are about -13, -15, -14.5 dBm for the PAR values of 0.16, 0.25, 0.36, respectively using the SIC-based Rx, which drops by about 4, 3, 2.5 dB for the CNN-based Rx.

Figure 7 shows the average BER performance as a function of P_r for downstream NOMA-PON using SIC- and CNN-based Rxs following transmission over a 40 km SMF with a PAR of 0.25

Optics EXPRESS

Table 1. System parameters.

Parameter	Value
Total data rate	11.7 Gbps
DFT and CP	64 and 8
Modulation –OFDM	4-QAM
RF carrier frequency	2.5 GHz
MZM	
3 dB bandwidth	10 GHz
Half-wave voltage	4.6 V
Insertion Loss	3.2 dB
Bias voltage	2.5 V
Operating wavelength	1525-1565 nm
Distributed feedback laser	
Wavelength	1550 nm
Transmit power	0, 10 dBm
SMF	
Length	20, 40 km
Dispersion	16e-6 s/m^2
Loss	0.2 dB/km
Optical Rx (Gooch & Housego)	
PD's responsibility@1550 nm	0.87 A/W
Bandwidth	~10 GHz

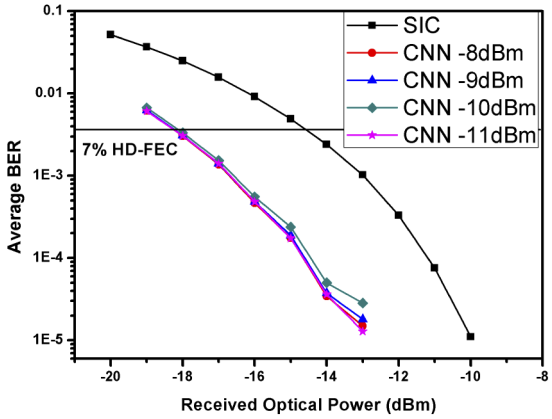

Fig. 4. BER performance vs. the received power after 20 km SMF for the PAR value of 0.16.

Optics EXPRESS

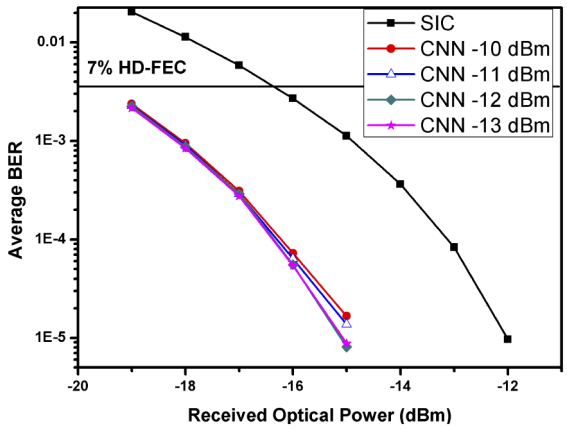

Fig. 5. BER performance vs. the received power after 20 km SMF for the PAR value of 0.25.

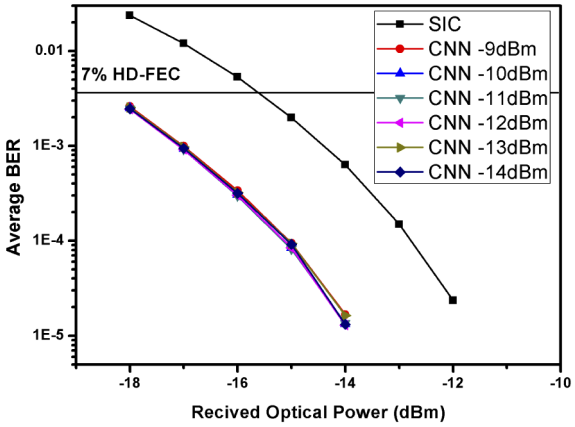

Fig. 6. BER performance vs. the received power after 20 km SMF for the PAR value of 0.36.

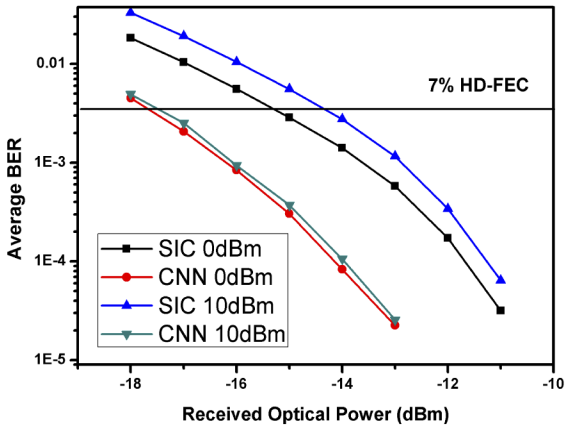

Fig. 7. BER performance vs. the received power for a 40 km SMF and a PAR of 0.25.

Optics EXPRESS

and P_t of 0 and 10 dBm. The CNN was trained for the P_r of -10 dBm. Increasing both P_t and the fiber length has more impact on NOMA-PON due to higher levels of nonlinear distortions. At the 7% hard-decision forward error correction (HD-FEC) BER limit of 3.8×10^{-3}, increasing P_t by 10 dB results in power penalties of about 1 and 0.1 dB for the SIC- and CNN-based Rxs, respectively. This is because the CNN based receiver can perform both linear and nonlinear compensation. Therefore, the proposed CNN based demodulator has high robustness again nonlinearity.

4. Conclusions

We proposed a CNN-based demodulator for NOMA-PON, where the multiplexed signal was decoded in a single-shot process with no channel estimation explicitly. The CNN with generalization ability was trained using the captured NOMA symbol at a given received optical power offline and used to direct online recovery of the transmitted data bit streams. We showed by experimental investigation that, the CNN-based Rx offered improved BER perofrmance and higher robustness against nonlinear distortion compared with the SIC-based Rx. After 20 km SMF transmission, the performance gains were 4, 3 and 2.5 dB for PARs of 0.16, 0.25, 0.36, respectively. With the increase of transmit optical power (i.e., more distortion induced by fiber nonlinearity), the BER performance for SIC significantly decreased compared to the proposed Rx.

Funding

Scientific Research Instrument and Equipment of CAS (YJKYYQ20170052); Science and Technology Program of Quanzhou (2019C010R); State Key Laboratory of Advanced Optical Communication Systems and Networks.; Fujian Provincial Department of Science and Technology (2017I0020); Sichuan Province Science and Technology Support Program (20SYSX0313); Haixi Institute, Chinese Academy of Sciences (Chunmiao Project).

Disclosures

The authors declare no conflicts of interest.

References

1. L. Dai, B. Wang, Y. Yuan, S. Han, I. Chih-Lin, and Z. Wang, "Non-orthogonal multiple access for 5G: solutions, challenges, opportunities, and future research trends," IEEE Commun. Mag. **53**(9), 74–81 (2015).
2. H. Huang, J. Xiong, J. Yang, G. Gui, and H. Sari, "Rate Region Analysis in a Full-Duplex-Aided Cooperative Nonorthogonal Multiple-Access System," IEEE Access **5**, 17869–17880 (2017).
3. Z. Wei, D. W. K. Ng, J. Yuan, and H. M. Wang, "Optimal Resource Allocation for Power-Efficient MC-NOMA with Imperfect Channel State Information," IEEE Trans. Commun. **65**(9), 3944–3961 (2017).
4. Z. Yang, C. Pan, W. Xu, and M. Chen, "Compressive Sensing-Based User Clustering for Downlink NOMA Systems With Decoding Power," IEEE Signal Process. Lett. **25**(5), 660–664 (2018).
5. Q. Wu, Z. Feng, M. Tang, X. Li, M. Luo, H. Zhou, S. Fu, and D. Liu, "Digital Domain Power Division Multiplexed Dual Polarization Coherent Optical OFDM Transmission," Sci. Rep. **8**(1), 15827 (2018).
6. B. Lin, W. Ye, X. Tang, and Z. Ghassemlooy, "Experimental demonstration of bidirectional NOMA-OFDMA visible light communications," Opt. Express **25**(4), 4348–4355 (2017).
7. X. Guan, Y. Hong, Q. Yang, and C. C.-K. Chan, "Non-orthogonal multiple access with phase pre-distortion in visible light communication," Opt. Express **24**(22), 25816–25823 (2016).
8. B. Lin, Z. Ghassemlooy, X. Tang, Y. Li, and M. Zhang, "Experimental demonstration of an NOMA-PON with single carrier transmission," Opt. Commun. **396**, 66–70 (2017).
9. B. Lin, J. Xu, Z. Ghassemlooy, and X. Tang, "Power-code division non-orthogonal multiple access scheme for next generation passive optical networks," Opt. Express **27**(24), 35740–35749 (2019).
10. F. Lu, M. Xu, L. Cheng, J. Wang, and G. Chang, "Power Division Non-Orthogonal Multiple Access (NOMA) in Flexible Optical Access with Synchronized Downlink / Asynchronous Uplink," J. Lightwave Technol. **35**(19), 4145–4152 (2017).
11. H. Li, Z. Huang, Y. Xiao, S. Zhan, and Y. Ji, "Solution for error propagation in a NOMA-based VLC network: symmetric superposition coding," Opt. Express **25**(24), 29856–29863 (2017).

Optics EXPRESS

12. C. Chen, W. Zhong, H. Yang, P. Du, and Y. Yang, "Flexible-Rate SIC-Free NOMA for Downlink VLC Based on Constellation Partitioning Coding," IEEE Wireless Commun. Lett. **8**(2), 568–571 (2019).
13. Y. Tan, J. Zhou, and J. Qin, "Novel Channel Estimation for Non-orthogonal Multiple Access systems," IEEE Signal Process. Lett. **23**(12), 1781–1785 (2016).
14. F. N. Khan, K. Zhong, X. Zhou, W. H. Al-Arashi, C. Yu, C. Lu, and A. P. T. Lau, "Joint OSNR monitoring and modulation format identification in digital coherent receivers using deep neural networks," Opt. Express **25**(15), 17767–17776 (2017).
15. S. Zhang, F. Yaman, K. Nakamura, T. Inoue, V. Kamlov, L. Jovanovski, V. Vusirikala, E. Mateo, Y. Inada, and T. Wang, "Field and lab experimental demonstration of nonlinear impairment compensation using neural networks," Nat. Commun. **10**(1), 3033 (2019).
16. L. Yi, T. Liao, L. Huang, L. Xue, P. Li, and W. Hu, "Machine Learning for 100 Gb/s/λ Passive Optical Network," J. Lightwave Technol. **37**(6), 1621–1630 (2019).
17. X. Lu, C. Lu, W. Yu, L. Qiao, S. Liang, A. P. T. Lau, and N. Chi, "Memory-controlled deep LSTM neural network post-equalizer used in high-speed PAM VLC system," Opt. Express **27**(5), 7822–7833 (2019).
18. G. Gui, H. Huang, Y. Song, and H. Sari, "Deep Learning for an Effective Nonorthogonal Multiple Access Scheme," IEEE Trans. Veh. Technol. **67**(9), 8440–8450 (2018).
19. N. Wu, X. Wang, B. Lin, and K. Zhang, "A CNN-Based End-to-End Learning Framework Toward Intelligent Communication Systems," IEEE Access **7**, 110197–110204 (2019).